Generation and Mesolysis of $PhSeSiR_3]^{\bullet-}$: Mechanistic Studies by Laser Flash Photolysis and Application for Bimolecular Group Transfer Radical Reactions†

Ganesh Pandey,*,‡ K. S. Sesha Poleswara Rao,‡ D. K. Palit,§ and J. P. Mittal*,§,⊥

Division of Organic Chemistry (Synthesis), National Chemical Laboratory, Pune-411 008, India, and Chemistry Division, Bhabha Atomic Research Center, Mumbai-400 085, India

Received December 31, 1997

Abstract: The investigation presented in this paper explores the mechanistic aspects and synthetic potentials of PET promoted reductive activation of selenosilane **1a** to its radical anion **1a**$^{\bullet-}$. PET activation of **1a** is achieved through a photosystem comprising a light-absorbing electron-rich aromatic (ERA), such as DMN or DMA, as an electron donor and ascorbic acid as a co-oxidant. The evidence for the ET from excited singlet states of DMN as well as DMA to **1a** is suggested by estimating negative ΔG_{et} (−51 and −43.46 kcal mol^{-1}, respectively) values and nearly diffusion-controlled fluorescence quenching rate constants (k_qTR) 0.36×10^{10} M^{-1} s^{-1} and 0.28×10^{10} M^{-1} s^{-1}, respectively, from time-resolved fluorescence quenching study. The transient absorption spectra of DMN$^{\bullet+}$, DMA$^{\bullet+}$, and **1a**$^{\bullet-}$ are obtained initially by pulse radiolysis in order to correlate the time-resolved absorption spectral data. Laser flash photolysis studies in the nanosecond time domain have confirmed the generation of **1a**$^{\bullet-}$, DMN$^{\bullet+}$, and DMA$^{\bullet+}$, supporting the participation of the triplet state of DMN or DMA in the ET reaction. Mesolytic cleavage of **1a**$^{\bullet-}$ produced a silyl radical and a phenyl selenide anion. The preparative PET activation of **1a** in acetonitrile in the presence of DMN or DMA leads to the formation of **5** and **6**, confirming the fragmentation pattern of **1a**$^{\bullet-}$. The overall ET rate constants (k_r(DMN) = 0.99×10^{10} M^{-1} s^{-1} and k_r(DMA) = 1.62×10^{10} M^{-1} s^{-1}) and limiting quantum yields (ϕ_{lim}(DMN) = 0.034 and ϕ_{lim}(DMA) = 0.12) are estimated from the inverse plot (1/[**1a**] vs 1/ϕ_{dis}) obtained by measuring the dependence of photodissociation quantum yields of **1a** at its maximum concentration in the presence of DMN or DMA. Silicon-centered radical species generated from the mesolysis of **1a**$^{\bullet-}$ are utilized for initiating a radical reaction by the abstraction of halogen atom from −C−X (X = Cl, Br) bonds, while PhSe$^-$ terminates the radical sequences via PhSeSePh. This concept is successfully applied for the bimolecular group transfer (BMGT) radical reactions and intermolecular radical chain addition reactions.

Introduction

Radical ions have emerged as critical intermediates in the development of modern organic reactivity concept.[1,2] Fragmentation of radical ions (mesolysis[3]) plays a major role in governing the chemoselectivity and efficiency of a wide variety of redox processes. Therefore, knowledge regarding the dynamics of mesolytic reactions is crucial to the design of an efficient and useful organic synthetic reaction. Generation of radical ions by photosensitized electron transfer (PET) processes has acquired prominence in the past decade,[4,5] as photoexcitation easily renders well-defined redox potential differences between interacting substrates—a prerequisite for an electron to exchange. The exchange of electron follows the free-energy gap law,[6] and the generation of free-radical ion pairs (FRIP) occurs via geminate radical ion pairs.[7] The mesolysis of these high-energy odd-electron species have afforded the means to apply PET reactions to drive energetically uphill processes in chemical synthesis[8−10] and energy conservation.[7a,b,11]

Interesting and synthetically useful chemistry has developed from the mesolysis of PET-generated radical cations.[8−10] Fragmentation of radical cations is generally associated with the deprotonation,[12−14] carbon−carbon,[15,16] and carbon−heteroatom[17,18] bond scission, rearrangements,[19] and addition to unsaturated bonds[20,21] in the primary event of PET processes. Mesolysis of radical cations from group IVA organometallics (−CMR_3; M = Pb, Sn, Si, Ge) is generally accompanied by the loss of

* To whom the correspondence should be addressed. Fax: 91-212-335153. E-mail: pandey@ems.ncl.res.in.

† Dedicated with respect to Dr. S. Rajappa on the occasion of his 65th birthday.

‡ National Chemical Laboratory.

§ Bhabha Atomic Research Center.

⊥ Also affiliated with Jawaharlal Nehru Center for Advanced Scientific Research, Banglore, as Honorary Professor.

(1) Kochi, J. K. *Angew. Chem., Int. Ed. Engl.* **1988**, *21*, 1227.

(2) Pross, A. *Adv. Phys. Org. Chem.* **1985**, *21*, 99. (b) Pross. A.; Shaik, S. S. *Acc. Chem. Res.* **1983**, *16*, 363.

(3) (a) Maslak, P.; Chapman, W. H.; Vallombroso, T. M., Jr.; Watson, B. A. *J. Am. Chem. Soc.* **1995**, *117*, 12380. (b) Maslak, P.; Narvaez, J. N.; Vallombroso, T. M., Jr. *ibid.* **1995**, *117*, 12373.

(4) Fox, M. A.; Chanon, M. D. *Photoinduced Electron Transfer*; Elsevier: Amsterdam, 1988; Parts A−D. (b) Fox, M. A. *Adv. Photochem.* **1986**, *13*, 295.

(5) Mattes, S. L.; Farid, S. In *Organic Photochemistry*; Padwa, A., Ed.; Marcel Dekker: New York, 1983; Vol. 6, p 233. (b) Davidson, R. S. *Adv. Phys. Org. Chem.* **1983**, *19*, 1. (c) Kavarnos, G. J.; Turro, N. J. *Chem. Rev.* **1986**, *86*, 401. (d) Julliard, M.; Chanon, M. *Ibid.* **1983**, *83*, 425.

(6) Weller, A. *Z. Phys. Chem. (Wiesbaden)* **1983**, *133*, 93. (b) Weller, A. *Ibid.* **1982**, *130*, 129. (c) Rhem, D.; Weller, A. *Isr. J. Chem.* **1970**, *8*, 259.

(7) (a) Gould, I. R.; Moser, J. E.; Armitage, B.; Farid, S. *Res. Chem. Intermed.* **1995**, *21*, 793. (b) Mattes, S. L.; Farid, S. *Science* **1984**, *226*, 917. (c) Gould, I. R.; Ege, D.; Moser, J. E.; Farid, S. *J. Am. Chem. Soc.* **1990**, *112*, 4290. (d) Mataga, N.; Okada, T.; Kanda, Y. Shioyama, H. *Tetrahedron* **1986**, *42*, 6143. (e) Masuhara, H.; Mataga, N. *Acc. Chem. Res.* **1981**, *14*, 312.

S0022-3263(97)02345-1 CCC: $15.00
Published on Web 05/15/1998

metal cations (MR_3^+) generating carbon-centered radicals,[22] with the exception of $-C-Se-]^{\bullet+}$ and $-C-S-]^{\bullet+}$, which produced carbocation.[23] Mesolyses of $Me_3Sn-MMe_3]^{\bullet+}$ (M = Sn, Ge, Si) and $Me_3Si-SiR_3]^{\bullet+}$ are also reported.[24−26] However, to the best of our knowledge, no report is available on the generation and fragmentation of radical anions from M−M bonds. It may be mentioned that the chemistry from the mesolysis of radical anions in general has remained unexplored, despite its great mechanistic and synthetic significance in organic chemistry.[27−29]

We have recently studied the PET generation and mesolysis of $-C-Se-]^{\bullet-}$ and reported[30] that the fragmentation of such species leads to the generation of carbon-centered radicals (Scheme 1, eq 1). Since carbon and silicon are isoelectronic and often predictions on the physical and chemical properties of silicon compounds are made by the direct analogy with what occurs in carbon chemistry, though the similarity between carbon and silicon to a great extent is only formal,[31−33] we became interested in exploring the chemistry of $-Si-Se-]^{\bullet-}$ species (Scheme 1, eq 2). We disclose herein the full details[34] of the PET reductive activation of selenosilanes (**1**), delineation of the mechanistic features of primary electron transfer (ET) processes by laser flash photolysis experiments, mesolytic pattern of $-Si-Se-]^{\bullet-}$, and the application of this chemistry for bimolecular group transfer (BMGT)[35] radical reactions and intermolecular radical chain transfer addition reactions. To the best of our knowledge, this study is the first of its own kind in the area of PET reductive activations and mesolysis of M−M bond compounds.

Scheme 1

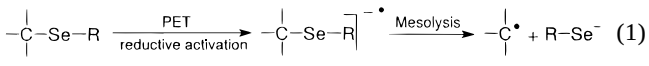

Scheme 2

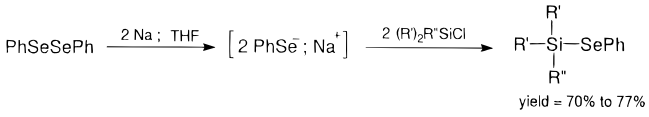

1a. R' = Ph ; R" = *t*Bu **1c.** R' = Me ; R" = *t*Bu

1b. R' = Me ; R" = Me **1d.** R' = Et ; R" = Et

Results and Discussion

For studying the mesolysis of $-Si-Se-]^{\bullet-}$, selenosilanes of type **1** were selected. These compounds (**1a**−**d**) were prepared[36] in 70−77% yield by the nucleophilic displacement of chloride ion of the corresponding R_3SiCl by in situ generated phenylselenide anion (Scheme 2).

The rate of chloride ion displacement by phenyl selenide anion decreases as the steric bulk around silicon increases.[33,36] Among the compounds **1a**−**d**, *tert*-butyl diphenyl(phenylseleno)silane (**1a**) was found to be the most stable and could be easily handled in aqueous solvents. Selenosilanes **1b**−**d** were highly susceptible to air and hydrolyzed to give the corresponding disiloxane (**2**) and phenylselenol (**3**) as shown in Scheme 3. There-

(8) (a) Mattay, J. *Synthesis* **1989**, 233. (b) Mattay, J. *Angew. Chem., Int. Ed. Engl.* **1987**, *26*, 825.
(9) Mariano, P. S.; Stavinoha, J. L. In *Synthetic Organic Photochemistry*; Horspool, W. M., Ed.; Plenum Press: London, 1983; p 145.
(10) (a) Pandey, G. In *Photoinduced Redox Reactions in Organic Synthesis in Molecular and Supramolecular Chemistry*; Ramamurthy, V., Ed.; Marcel Dekker, Inc.: New York, 1997; Vol. 2, Chapter 7, p 245. (b) Pandey, G. *Top. Curr. Chem.* **1993**, *168*, 175. (c) Pandey, G. *Synlett* **1992**, 546.
(11) (a) Willner, I.; Willner, B. *Top. Curr. Chem.* **1981**, *159*, 157 and references therein. (b) Webber, S. E. *Chem. Rev.* **1990**, *90*, 1469. (c) Gust, D.; Moore, T. A. *Top. Curr. Chem.* **1990**, *159*, 103. (d) Gust, D.; Moore, T. A.; Moore, A. L. *Acc. Chem. Res.* **1993**, *26*, 198.
(12) (a) Baciocchi, E.; Del Giacco, T.; Elisei, F. *J. Am. Chem. Soc.* **1993**, *115*, 5, 12290. (b) Parker, V. D.; Tilset, M. *J. Am. Chem. Soc.* **1991**, *113*, 8778. (c) Parker, V. D.; Chao, Y.; Reitstoen, B. *Ibid.* **1991**, *113*, 2336. (d) Reitstoen, B.; Parker, V. D. *Ibid.* **1990**, *112*, 4968.
(13) Schlesener, C. J.; Amatore, C.; Kochi, J. K. *J. Am. Chem. Soc.* **1984**, *106*, 6, 7472.
(14) Dinnocenzo, J. P.; Banach, T. E. *J. Am. Chem. Soc.* **1989**, *111*, 8646.
(15) (a) Maslak, P.; Narvaez, J. N.; Vallombroso, T. M., Jr. *Angew. Chem., Int. Ed. Engl.* **1994**, *33*, 73. (b) Maslak, P. *Top. Curr. Chem.* **1993**, *168*, 1.
(16) (a) Sankararaman, S.; Perrier, S.; Kochi, J. K. *J. Chem. Soc., Perkin Trans. 2* **1993**, 825. (b) Sankararaman, S.; Perrier, S.; Kochi, J. K. *J. Am. Chem. Soc.* **1989**, *111*, 6448.
(17) (a) Zhang, X.; Yeh, S. R.; Hong, S.; Freccero, M.; Albini, A.; Mariano, P. S. *J. Am. Chem. Soc.* **1994**, *116*, 4211. (b) Yoon, U. C.; Mariano, P. S. *Acc. Chem. Res.* **1992**, *25*, 233.
(18) Johnston, L. J.; Kwong, P.; Shelemay, A.; Lee-Ruff, E. *J. Am. Chem. Soc.* **1993**, *115*, 1664.
(19) (a) Weng, X.; Sheik, Q.; Roth, H. D. *J. Am. Chem. Soc.* **1995**, *117*, 10655. (b) Weng, X.; Du, X.-M.; Roth, H. D. *Ibid.* **1995**, *117*, 135. (c) Ishiguro, K.; Turro, N. J.; Roth, H. D. *Ibid.* **1994**, *116*, 6933. (d) Roth, H. D.; Herbertz, T. *Ibid.* **1993**, *115*, 9801.
(20) Horner, J. H.; Martinez, F. N.; Musa, O. M.; Newcomb, M.; Shain, H. E. *J. Am. Chem. Soc.* **1995**, *117*, 11124.
(21) Mirafzal, G. A.; Kim, T.; Liu, J.; Bauld, N. L. *J. Am. Chem. Soc.* **1992**, *114*, 10968.
(22) (a) Kochi, J. K. *Organometallic Mechanisms and Catalysis*; Academic Press: New York, 1978; pp 445−499. (b) Symons, M. C. R. *Chem. Soc. Rev.* **1984**, *13*, 393. (c) Eaton, D. F. *J. Am. Chem. Soc.* **1981**, *103*, 7235. (d) Pandey, G.; Kumaraswamy, G.; Bhalerao, U. T. *Tetrahedron Lett.* **1989**, *30*, 6059.
(23) (a) Pandey. G.; Soma Sekhar, B. B. V. *J. Org. Chem.* **1994**, *59*, 7367. (b) Pandey, G.; Soma Sekhar, B. B. V.; Bhalerao, U. T. *J. Am. Chem. Soc.* **1990**, *112*, 5650. (c) Platen, M.; Steckhan, E. *Liebigs. Ann. Chem.* **1984**, 1563.
(24) (a) Fukuzumi, S.; Kitano, T. *J. Am. Chem. Soc.* **1990**, *112*, 3246. (b) Fukuzumi, S.; Kitano, T.; Mochida, K. *J. Chem. Soc., Chem. Commun.* **1990**, 1236.
(25) (a) Mochida, K.; Itani, A.; Yokayama, M.; Tsuchiya, T.; Worley, S. D.; Kochi, J. K. *Bull. Chem. Soc. Jpn.* **1985**, *58*, 2149. (b) Mochida, K.; Worley, S. D.; Kochi, J. K. *Ibid.* **1985**, *58*, 3389. (c) Walther, B. W.; Williams, F.; Lau, W.; Kochi, J. K. *Organometallics* **1983**, *2*, 688.
(26) Wang, J. T.; Williams, F. *J. Chem. Soc., Chem. Commun.* **1981**, 666.
(27) (a) Guthrie, R. D.; Patwardhan, M.; Chateauneuf, J. E. *J. Phys. Org. Chem.* **1994**, *7*, 147. (b) Wu, F.; Guarr, T. F.; Guthrie, R. D. *Ibid.* **1992**, *5*, 7.
(28) (a) Masnovi, J. *J. Am. Chem. Soc.* **1989**, *111*, 9081. (b) Saeva, F. D. *Tetrahedron* **1986**, *42*, 6132. (c) Koppang, M.; Woolsey, N. F.; Bartak, D. E. *J. Am. Chem. Soc.* **1984**, *106*, 2799.
(29) Andrieux, C. P.; Gorande, A. L.; Saveant, J.-M. *J. Am. Chem. Soc.* **1992**, *114*, 6892. (b) Mautner, M.; M.-N.; Neta, P.; Norris, R. K.; Wilson, K. *J. Phys. Org. Chem.* **1986**, *90*, 168. (c) Ruhl, J. C.; Evans, D. H.; Hapiot, P.; Neta, P. *J. Am. Chem. Soc.* **1991**, *113*, 5188.
(30) (a) Pandey, G.; Sesha Poleswara Rao, K. S.; Nageshwar Rao, K. V. *J. Org. Chem.* **1996**, *61*, 6799. (b) Pandey, G.; Sesha Poleswara Rao, K. S.; Soma Sekhar, B. B. V. *J. Chem. Soc., Chem. Commun.* **1993**, 1636.
(31) (a) West, R.; Carberry, E. *Science* **1975**, *189*, 179. (b) West, R.; Carberry, E. *Pure Appl. Chem.* **1982**, *54*, 1041.
(32) Tandura, N.; Alekseev, N. V.; Voronkov, M. G. *Top. Curr. Chem.* **1986**, *131*, 101 and references therein.
(33) MacDiarmid, A. G. *Advances in Inorganic Chemistry and Radiochemistry*; 1961; Vol. 3, p 207 and references therein.
(34) Pandey, G.; Sesha Poleswara Rao, K. S. *Angew. Chem., Int. Ed. Engl.* **1995**, *34*, 2669.
(35) Analogous to BMGT, the term UMGT (unimolecular group transfer) has been introduced recently by us.[30a] Curran et al. have also used the term UMCT (unimolecular chain transfer) for radical chain reactions. (a) Curran, D. P.; Jinyou, Xu. *J. Chem. Soc., Perkin Trans. 1* **1995**, *24*, 3061. (b) Curran, D. P.; Jinyou, Xu.; Lazzarini, E. *Ibid.* **1995**, *24*, 3049. (c) Curran, D. P.; Jinyou, Xu.; Lazzarini, E. *J. Am. Chem. Soc.* **1995**, *117*, 6603.
(36) Detty, M. R. *J. Org. Chem.* **1981**, *46*, 1283.

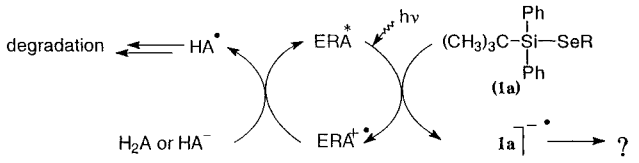

Figure 1. Photosystem for PET reductive activation.

Scheme 3

$$\underset{\textbf{(1b-1d)}}{PhSeSiR_3} \xrightarrow[\text{or aq. solvent}]{MeOH} \underset{\textbf{2}}{R_3SiOSiR_3} + \underset{\textbf{3}}{PhSeH} \xrightarrow{oxd.} PhSeSePh$$

fore, we elected to use **1a** as a representative selenosilane to study the PET reductive activation of −Si−Se− bonds.

(A) PET Reductive Activation of 1a: Photophysical Studies

To generate radical anions from −Si−Se− bond compounds (selenosilane **1a**), a photosystem comprising electron-rich aromatics (ERA) such as 1,5-dimethoxynaphthalene (DMN) or 9,10-dimethoxyanthracene (DMA) as the light-harvesting electron donor and ascorbic acid as the sacrificial electron donor was utilized as shown in Figure 1.

(i) Thermodynamic Parameters. The thermodynamic feasibility of ET between ERA and **1a** was first deduced by estimating the Gibbs free energy change (ΔG_{et}) for radical ion formation using the Weller equation[6c] (eq 3), where $E_{1/2}^{ox.}$[D] is the oxidation potential of ERA,

$$\Delta G_{et} = E_{1/2}^{ox.}[D] - E_{1/2}^{red.}[A] - E_{exc}[D] \qquad (3)$$

$E_{1/2}^{red.}$[A] is the reduction potential of **1a**, and E_{exc}[D] is the excitation energy of ERA. Substituting eq 3 with the appropriate values of $E_{1/2}^{red.}$ of **1a** (0.344 eV/SCE), obtained by cyclic voltammetry (for details see the Experimental Section), $E_{1/2}^{ox.}$ of DMN (1.28 eV),[37] and excitation energy of DMN (87.8 kcal mol^{-1}),[37] an exoergic value of −51 kcal mol^{-1} was obtained. Similarly, ET feasibility from ascorbic acid to DMN$^{\bullet+}$ was evaluated by estimating ΔG_{et} (−4.51 kcal mol^{-1}) employing the equation $\Delta G_{et} = E_{1/2}^{ox.} - E_{1/2}^{red.}$. The $E_{1/2}^{ox.}$ value (1.084 eV/SCE) for ascorbic acid was estimated by cyclic voltammetry. The electron-donating ability of ascorbate ion and its transformation to dehydroascorbic acid and proton is precedented in the literature.[38] To achieve the PET reduction of **1a** by visible light irradiation, DMA (λ_{max} 380 and 425 nm, Figure 2C) was also evaluated as a potential electron donor. Accordingly, the ΔG_{et} value (−43.46 kcal mol^{-1}) for the ET between DMA and **1a** was estimated utilizing oxidation potential and singlet excitation energy values of DMA as 0.98 eV and 74 kcal mol^{-1}, respectively.[39] In a similar manner, the ΔG_{et} value for the ET from ascorbic acid to DMA$^{\bullet+}$ was also estimated to be −3.82 kcal mol^{-1}. The free energy change of ET from triplet states of ERA [ΔG_{et} (^{t}DMN) = −29.90 kcal mol^{-1}; ΔG_{et} (^{t}DMA) = −11.50 kcal mol^{-1}] were also estimated by taking the reported[39] values of triplet excitation energy and were found to be in the exoergic region.

(ii) Steady-State and Time-Resolved Fluorescence Quenching Studies. Preliminary information about the interaction of the excited singlet (S_1) state of DMN/DMA with **1a** was obtained from both steady-state as well as time-resolved fluorescence-quenching studies. Fluorescence lifetimes (τ) of DMN and DMA in deareated acetonitrile solution were determined to be 16.67 and 12.27 ns, respectively.[40] The fluorescence lifetimes of both DMN and DMA were seen to be heavily quenched by **1a** in acetonitrile solution. The Stern−Volmer (S−V) plots obtained from lifetime quenching studies were perfectly linear (Figure 3) throughout the range of concentrations of **1a**, and the quenching rate constants were determined to be k_qTR (DMN) = 0.36 × 10^{10} M^{-1} s^{-1} and k_qTR (DMA) = 0.28 × 10^{10} M^{-1} s^{-1}, respectively. Steady-state fluorescence quenching of DMN (λ_{exi} = 300 nm, λ_{emi} = 344 nm) or DMA (λ_{ex} = 410 nm; λ_{em} = 440 nm) by **1a** also obeyed S−V relation. From the slopes ($k_{qf} \times \tau$) of the straight lines (Figure 4) and singlet lifetimes of DMN and DMA, respectively, the quenching rate constants [k_{qf}SS (DMN) = 0.822 × 10^{10} M^{-1} s^{-1}, k_{qf}SS (DMA) = 1.46 × 10^{10} M^{-1} s^{-1}] were calculated and found to be near diffusion[5a] (k_{diff} = 2.30 × 10^{10} M^{-1} s^{-1}). Emission and excitation spectra of DMN and DMA remained unaffected in the presence of the maximum concentration of **1a** in acetonitrile. No exciplex emission was noticed in either polar (CH_3CN) or nonpolar (cyclohexane) solvents. However, the absorption values at the excitation wavelength were found to increase slightly with the increase in the concentration of the quencher (**1a**). The fluorescence quenching rate constants determined from the time-resolved studies are found to be lower than those obtained from steady state quenching analysis. This discrepancy in the rates could possibly be due to the static quenching by the absorption of excitation light by the quencher. Since in both time resolved (Figure 3) and steady state (Figure 4) fluorescence quenching studies the S−V plots obtained are perfectly linear, the possibility of exciplex formation or ground-state complexation can be excluded. Quenching due to heavy-atom-induced intersystem crossing could also be suggested to be minimal on the basis of similar logic as provided by Eaton et al.[22c] It is reasonable, therefore to assume that fluorescence quenching in these cases takes place due to the interaction of the excited singlet states of DMN and DMA with **1a** via a single electron-transfer mechanism.

(iii) Laser Flash Photolysis Studies: Evaluation of the Transient Species. To gain direct evidence of primary ET processes from the excited states of DMN or DMA to **1a** and also to observe the transient spectra of the radical ions thus formed, a laser flash photolysis study was undertaken. Since the absorption properties of the DMN$^{\bullet+}$, DMA$^{\bullet+}$, and **1a**$^{\bullet-}$ were not known, pulse

(37) Hamada, T.; Nishida, A.; Yonemitsu, O. *J. Am. Chem. Soc.* **1986**, *108*, 140.

(38) (a) Brown, G. M.; Brunschwig, B. S.; Creutz, C.; Endicott, J. F.; Sutin, N. *J. Am. Chem. Soc.* **1979**, *101*, 1298. (b) Bielski, B. H. J.; Comstock, D. A.; Bowen, R. A. *Ibid.* **1971**, *93*, 5624.

(39) (a) Zweig, A.; Maurer, A. H.; Roberts, B. G. *J. Org. Chem.* **1967**, *32*, 2, 1322. (b) Yeung, C. K.; Jasse, B. *Makromol. Chem.* **1984**, *185*, 541. (c) Lee, G. A.; Israel, S. H. *J. Org. Chem.* **1983**, *48*, 4557.

(40) The lifetime value (τ_{DMA}) obtained for DMA is in agreement with the value reported in the literature,[39] but the lifetime value (τ_{DMN}) for DMN is higher than the literature value (12.6 ns) as reported by Hamada et al.[37] Possibly, the lifetime value reported[37] for DMN is lower due to the presence of a trace amount of oxygen in the solution.

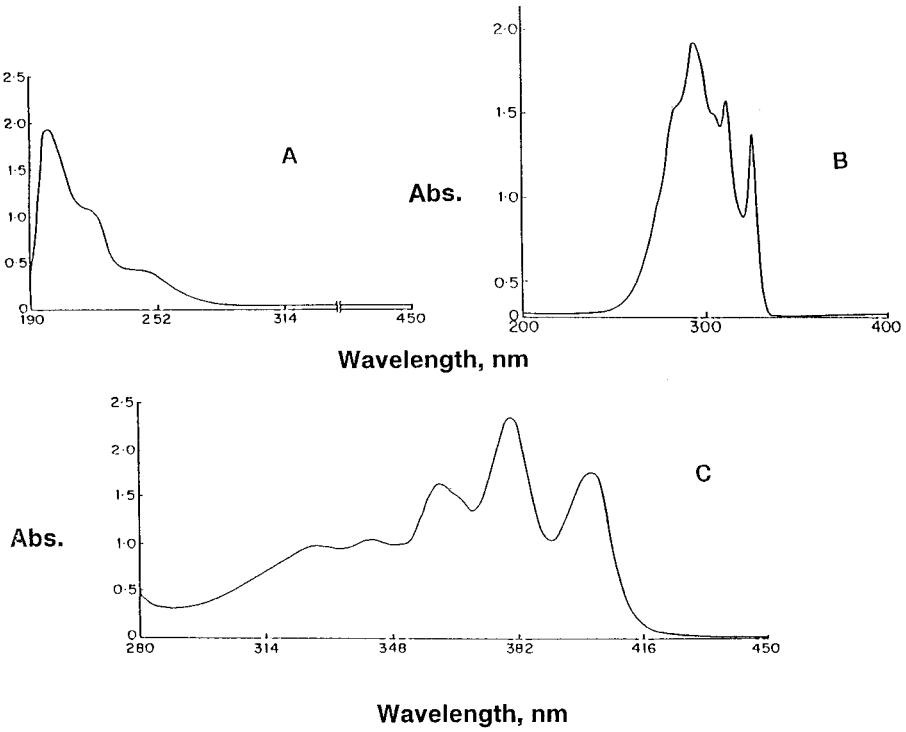

Figure 2. UV-absorption spectra of **1a** (0.003 M, A), DMN (0.0025 M, B), and DMA (0.0018 M, C).

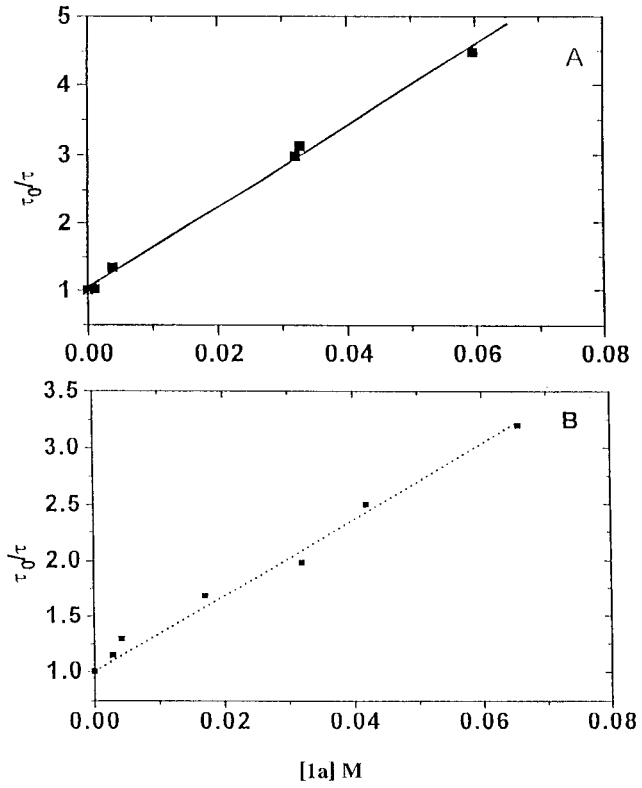

Figure 3. Stern−Volmer plots for time resolved fluorescence quenching for DMN (A) and DMA (B) by **1a** in CH_3CN solution.

radiolysis experiments were carried out at first individually.

$DMN^{\bullet+}$ or $DMA^{\bullet+}$ was generated indirectly by ET from DMN or DMA to the electron-deficient species $^{\bullet}CCl_3$, produced by the dissociation of $CCl_4^{\bullet-}$, formed by the capture of an electron from a high-energy electron pulse (Scheme 4).[41] The absorption spectra of $DMN^{\bullet+}$ and

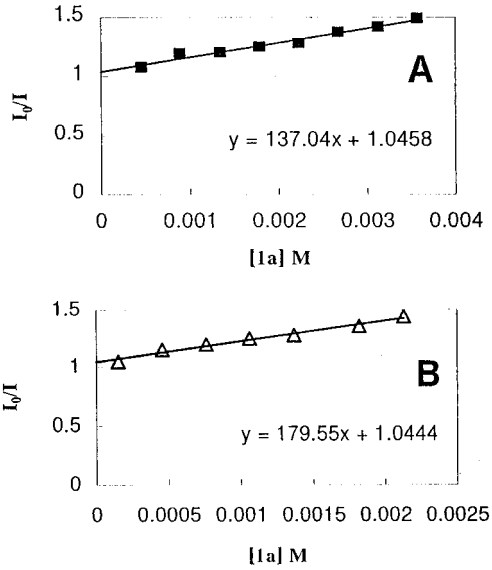

Figure 4. Stern−Volmer plots for steady-state fluorescence quenching for DMN (A, ■) and DMA (B, △) by **1a** in CH_3CN solution.

Scheme 4

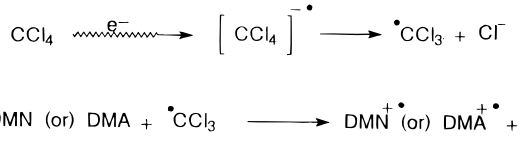

$DMA^{\bullet+}$, thus obtained are given in Figure 5A. $DMA^{\bullet+}$ has an absorption peak at 400 nm and shoulders at 450, 530, and 580 nm, whereas the absorption of $DMN^{\bullet+}$ extends from 400 to 700 nm without having any well-defined peak.

(41) Shida, T.; Haselbach, E.; Bally, T. *Acc. Chem. Res.* **1984**, *17*, 180 and references therein.

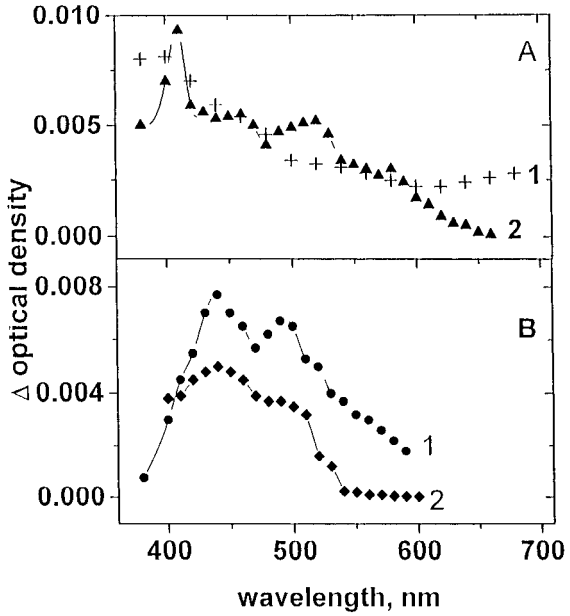

Figure 5. (A) Transient absorption spectra of $DMN^{\bullet+}$ (curve 1, +) and $DMA^{\bullet+}$ (curve 2, ▲) obtained by pulse radiolysis of DMN and DMA in CCl_4 solution. (B) Transient absorption spectra obtained by pulse radiolysis (curve 1, ●) and flash photolysis (curve 2, ◆) of **1a** in CH_3CN solution.

Scheme 5

$$PhSeSiR_3\ (\mathbf{1a}) \xrightarrow[CH_3CN]{e^-} [\mathbf{1a}]^{-\bullet} \xrightarrow{\text{mesolysis}} \underset{(440\ nm)}{R_3Si^{\bullet}} + \underset{(490\ nm)}{PhSe^-}$$

The transient absorption spectrum (Figure 5B, curve 1) obtained due to pulse radiolysis of **1a** in acetonitrile has two absorption maxima at 440 and 490 nm, suggesting that highly unstable $\mathbf{1a}^{\bullet-}$ possibly dissociates efficiently to some other species (Scheme 5).

To gather evidence of $\mathbf{1a}^{\bullet-}$ dissociating into the corresponding $R_3Si^{\bullet}$ and $PhSe^-$, a homolysis experiment of **1a** with higher concentration (0.09 M) in acetonitrile using 355 nm light from a Nd:YAG laser was undertaken. The absorption spectrum (Figure 5B, curve 2) of the transient species showed a well-defined peak at 440 nm with a shoulder at 510 nm. Homolysis of **1a** was expected to produce $R_3Si^{\bullet}$ and $PhSe^{\bullet}$ species. The transient absorption at 440 nm could be assigned to the silyl radical species on the basis of literature data.[42a] Therefore, the other transient absorption at 510 nm may be assigned to the phenylselenyl radical ($PhSe^{\bullet}$). The transient absorption of $PhSe^{\bullet}$ at 510 nm has been further confirmed by the homolysis experiment of PhSeSePh using 355 nm light pulses.[42b] Since not much change in the UV absorption spectrum (200−450 nm) of **1a** before and after irradiation at 355 nm was observed, the possibility of a faster rate of geminate radical recombination compared to their dissociation rate was obvious (Scheme 6).

On the basis of the above experiments, it may, thus, be pointed out that $\mathbf{1a}^{\bullet-}$, produced by the pulse radiolysis, dissociates into the corresponding silyl radical (440 nm) and phenylselenide anion (490 nm) (Scheme 5).

(iv) Picosecond Laser Flash Photolysis. To observe possible generation of transient species $\mathbf{1a}^{\bullet-}$ and $DMA^{\bullet+}$ or $DMN^{\bullet+}$ during PET reaction, first we attempted to carry out a picosecond laser flash photolysis experiment on a mixture of DMA (OD = 0.6) and **1a** (0.03 M) in CH_3CN. The transient absorption spectrum of DMA in the picosecond time domain was recorded in the absence and presence of **1a**. The singlet−singlet (S−S) absorption spectrum (Figure 6, curve a) of DMA (in absence of **1a**) showed two peaks at 550 and 930 nm. Addition of 0.03 M of **1a** to DMA solution resulted in significant quenching (Figure 6, curve **b**) of the singlet of DMA. This indicated the possibility of an interaction between the singlet state of DMA and **1a**. The addition of a higher concentration (0.1 M) of **1a** to DMA solution resulted in the complete quenching of the excited singlet state of DMA (Figure 6, curve c). However, transient species absorption corresponding to either $DMA^{\bullet+}$ (460 nm) or $\mathbf{1a}^{\bullet-}$ (490 nm) could not be observed due to the low sensitivity of picosecond absorption technique below the 500 nm region where the $DMA^{\bullet+}$ has significant absorption and also possibly a very low quantum yield of the cation radical. Identical experiments conducted using DMN as sensitizer also could not show the $DMN^{\bullet+}$ transient absorption due to the same reason as mentioned above.

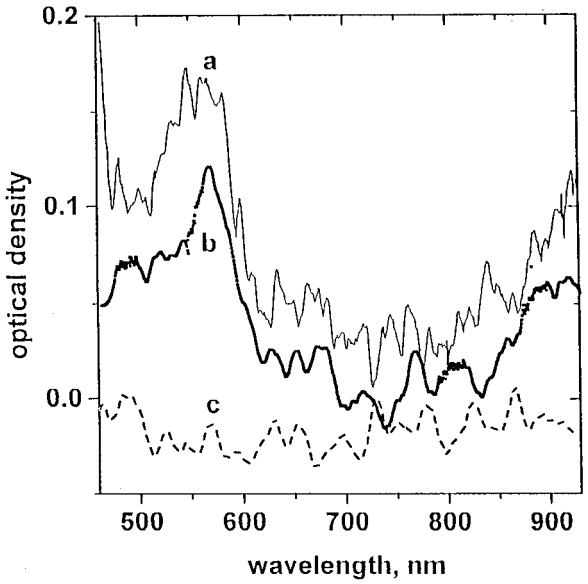

Figure 6. Singlet−singlet absorption spectra of DMA in the absence (a) and presence of 0.03 M (b) and 0.1 M (c) of **1a** in CH_3CN solution.

Scheme 6

$$PhSeSiR_3 \underset{\lambda = 355\ nm;\ CH_3CN}{\overset{h\nu}{\rightleftharpoons}} \underset{(440\ nm)}{R_3Si^{\bullet}} + \underset{(510\ nm)}{PhSe^{\bullet}}$$

Scheme 7

$$DMA + \mathbf{1a} \xrightarrow[CH_3CN]{h\nu\ \ \lambda = 355\ nm} {}^tDMA^* + DMA^{+\bullet} + [\mathbf{1a}]^{-\bullet}$$

(v) Nanosecond Laser Flash Photolysis. To gain possible evidence of interaction between the triplet states of DMN or DMA and **1a**, we undertook laser flash photolysis studies and lifetime measurements in the nanosecond time domain.

The triplet−triplet (T−T) absorption spectra of DMA (OD = 0.6) in acetonitrile solution were recorded in the nanosecond time domain. The absorption spectrum displayed a well-defined peak (λ_{max}) at 440 nm that extended up to 700 nm (Figure 7A, curve 1). The lifetime

(42) (a) Sluggett, G. W.; Leigh, W. J. *Organometallics* **1992**, *11*, 3731. (b) Palit, D. K.; Bhasikuttan, A. C.; Sapre, A. V. Unpublished results.

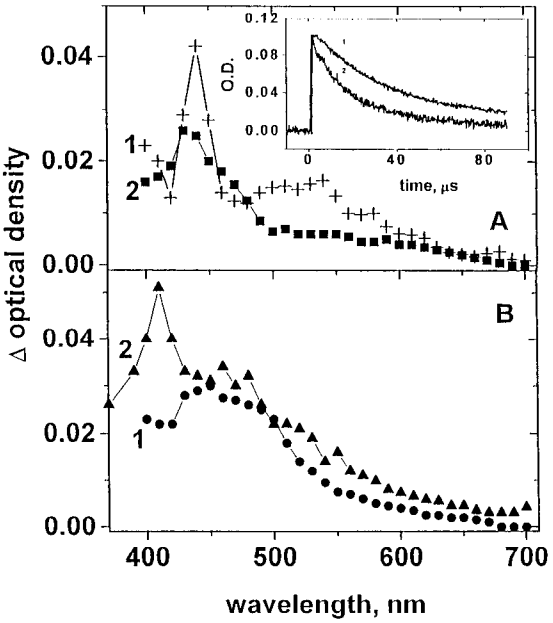

Figure 7. (A) Transient absorption spectra obtained by flash photolysis of DMA in CH_3CN in the absence (curve 1, T−T absorption spectra of DMA, +) and presence of 0.03 M of **1a** (curve 2, ■). Inset shows the decay traces monitored at 550 nm for only DMA (curve 1, $\tau = 33$ μs) and DMA + 0.03 M of **1a** (curve 2, $\tau = 25$ μs). (B) Transient absorption spectra obtained by laser flash photolysis of DMA in the presence of 0.05 M (curve 1, ●) and 0.09 M (curve 2, ▲) of **1a** in CH_3CN.

Scheme 8

$$DMA^{+\bullet} + BP \xrightarrow[CH_3CN]{h\nu \;\; \lambda = 355\ nm} DMA + BP^{+\bullet}$$

of the triplet state of DMA was determined to be 33 μs. Addition of **1a** (0.03 M) resulted in the quenching of the triplet state of DMA, and the lifetime of DMA was seen to decrease to 25 μs (Figure 7A, inset). This observation suggested the interaction of **1a** with the triplet excited state of DMA too.[43]

The shape of the T−T absorption spectrum obtained in the presence of 0.03 M concentration of **1a** was quite different from that of the original T−T absorption spectrum (Figure 7A, curve 2) of DMA. Kinetic analysis at 440 nm was complicated possibly due to the presence of more than one transient species, i.e., the triplet state of DMA, $DMA^{\bullet+}$, and $\mathbf{1a}^{\bullet-}$. However, kinetic analysis of the transient decay monitored at 550 nm revealed that the triplet lifetime of DMA had been quenched to 25 μs, indicating the interaction of the triplet state with **1a**. Monitoring the transient species after the addition of a higher concentration of **1a** (0.05 and 0.09 M, Figure 7B) in DMA (OD = 0.6) solution indicated the formation of $DMA^{\bullet+}$ (460 nm) and $\mathbf{1a}^{\bullet-}$ (440 nm). An indirect approach was also made to characterize the transient absorption species related to $DMA^{\bullet+}$ by the sensitized generation of $BP^{\bullet-}$ (750 nm) (Scheme 8); however, this attempt failed, possibly due to very low concentration of $DMA^{\bullet+}$ generated in the solution and, therefore, suggesting a very low quantum yield of the ^{t}DMA* electron-transfer channel.

A similar experiment was also carried out using DMN to monitor the corresponding transient species in the absence and presence of **1a**. Curve 1 in Figure 8 is the T−T absorption spectrum of DMN in CH_3CN. The lifetime of the ^{t}DMN* was determined to be 28 μs. Addition of 0.03 M of **1a** resulted in the quenching of the triplet state of DMN, and the lifetime of DMN was seen to decrease to 14 μs (Figure 8, inset). Addition of a higher concentration (0.09 M) of **1a** resulted in increased absorption in the wavelength region 500−650 nm (Figure 8, curve 3), providing an indication of the formation of $DMN^{\bullet+}$ in solution due to interaction between the DMN triplet state and **1a** via ET phenomena.

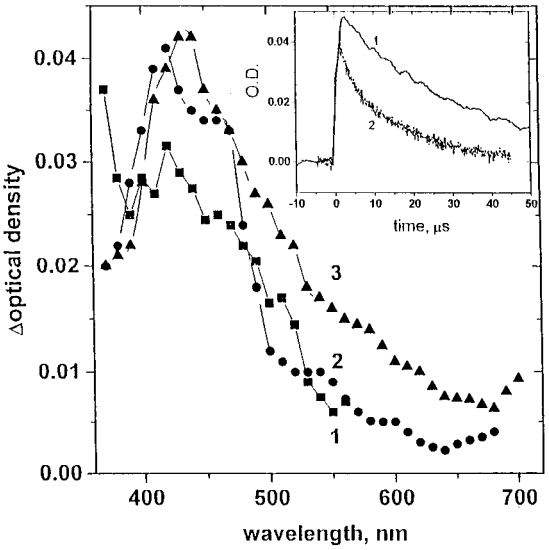

Figure 8. Transient absorption spectra obtained by laser flash photolysis of DMN in CH_3CN in the absence (curve 1, T−T absorption spectra of DMN, ■) and presence of 0.03 M (curve 2, ●) and 0.09 M (curve 3, ▲) of **1a**. Inset shows the transient decay monitored at 520 nm in the absence (curve 1, $\tau = 28$ μs) and presence (curve 2, $\tau = 14$ μs) of **1a**.

From the above steady-state and time-resolved fluorescence quenching studies and laser flash photolysis experiments, it is confirmed that the ET from the excited state of DMA or DMN (both singlet as well as triplet) to **1a** leads to the formation of $\mathbf{1a}^{\bullet-}$. However, due to strong overlapping of the absorption spectra of the transients produced, it has not been possible to comment on the relative yields of the two different channels (singlet and triplet) of the ET reaction. To support above photophysical observations and to study the mesolytic pattern of $\mathbf{1a}^{\bullet-}$, a preparative PET activation of **1a**, utilizing the photosystem as shown in Figure 1, was initiated.

(B) PET Activation of 1a: A Preparative Study

A dilute solution of acetonitrile containing a mixture of **1a** (0.3 mmol), DMN (0.1 mmol), and ascorbic acid (0.3 mmol) was irradiated through Pyrex-filtered light ($\lambda \geq 310$ nm) using a 450 W Hanovia medium-pressure lamp at room temperature. The progress of the reaction was monitored by HPLC (C_{18} reversed-phase column: CH_3CN/H_2O = 70:30) analysis. After 5 h of irradiation, when considerable consumption of **1a** was noticed, irradiation was discontinued and solvent was removed under vacuum. The crude reaction mixture was purified by column chromatography to give **5** and **6**. The products (**5** and **6**) were characterized by ^{1}H NMR and mass spectral data. DMN was recovered unchanged after the reaction in about 98% yield.

(43) Absence of curvature in the S−V plots (Figures 3 and 4) may possibly be due to very low quantum yield of electron-transfer channel available from the triplet state of the excited donor.

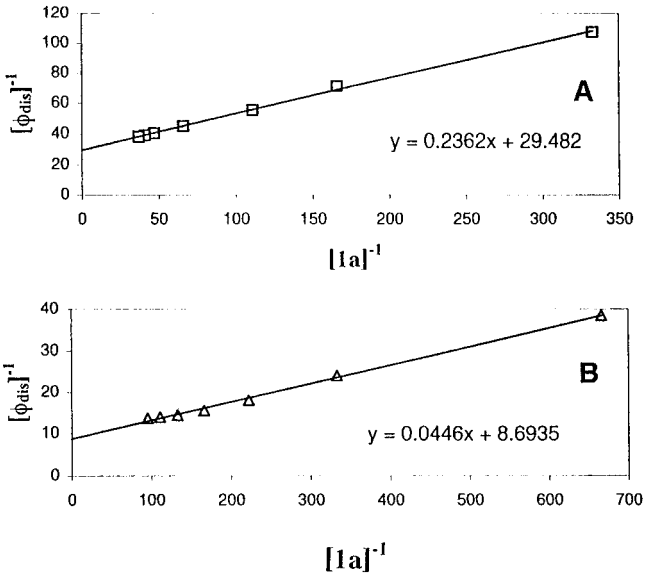

Figure 9. Inverse plot of $[\phi_{dis}]$ vs [**1a**] with DMN (A, □) and DMA (B, △).

Scheme 9

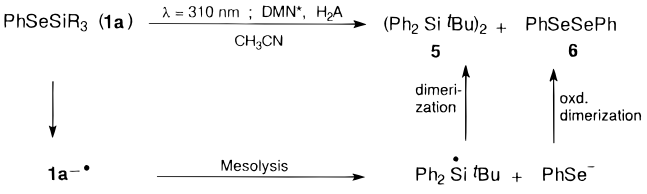

Mechanistically, the formation of **5** and **6** could be rationalized by implicating the mesolysis of the primary photoproduct **1a**$^{\bullet-}$ to $R_3Si^{\bullet}$ and $PhSe^-$. Subsequent dimerization of the silyl radical led to the formation of **5** while the diphenyl diselenide (**6**) is obtained either by the oxidative dimerization of the resultant phenyl selenide anion directly or via the phenylselenol produced by the protonation of $PhSe^-$. Thus, it appears that the electronegativity difference between selenium and silicon directs the fragmentation of **1a**$^{\bullet-}$ as shown in Scheme 9. The quantum yield (ϕ_{dis}(DMN)) for the disappearance of **1a** in the above reaction (Scheme 9) was estimated by photolyzing **1a** and DMN using 310 nm monochromatic light.[44] The value of ϕ_{dis}(DMN) was found to be 0.042.

To implicate steady-state photochemical reaction and photophysical observations through a common intermediate, a quantitative description was also derived by correlating the rates of fluorescence quenching (k_{qf}SS) and overall ET quenching rate constant (k_r) through a reciprocal plot (Figure 9A) of $1/\phi_{dis}$ vs $1/C$. The overall reaction rate constant k_r(DMN) = 0.991×10^{10} M^{-1} s^{-1} obtained from the reciprocal plot (Figure 9A) is in good correlation with the Stern−Volmer fluorescence quenching rate constant [k_{qf}SS(DMN) = 0.82×10^{10} M^{-1} s^{-1}]. The limiting quantum yield (ϕ_{lim}(DMN)) for overall reaction was found to be 0.034.

PET activation of **1a** by visible light (410 nm)[44] using DMA as the electron donor also led to the formation of **5** and **6** in more or less the same proportions. The quantum yield (ϕ_{dis}(DMA)) for the disappearance of **1a** with DMA was found[45] to be 0.223. Similar correlation studies, as described for DMN, gave k_r(DMA) as 1.62×10^{10} M^{-1} s^{-1} and ϕ_{lim}(DMA) as 0.12, respectively. The overall reaction rate (k_r(DMA); calculated from inverse plot, Figure 9B) was found to be in good agreement with the rate constant obtained from fluorescence quenching [k_{qf}SS(DMA) = 1.46×10^{10} M^{-1} s^{-1}].

Scheme 10

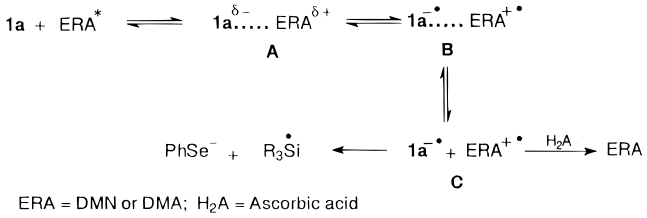

On the basis of the above observations, the present reaction could be summarized by considering single-electron transfer (SET) from the excited state of DMN* and DMA* (singlet as well as triplet) to **1a** via charge-transfer-stabilized exciplex intermediate (**A**). The intermediate **A** dissociates into a free-radical ion pair (FRIP, **C**) via the solvent-separated ion pair (SSIP, **B**) resulting in **1a**$^{\bullet-}$ and ERA$^{\bullet+}$ as anticipated in solvents of high dielectric constant. Fast disproportionation of **1a**$^{\bullet-}$ leads to the formation of $R_3Si^{\bullet}$ and $PhSe^-$ (Scheme 10).

(C) Synthetic Perspectives

It is evident from the steady-state and laser flash photolysis studies that photoexcitation of the DMN−**1a** pair facilitates one-electron exchange to produce **1a**$^{\bullet-}$ as well as DMN$^{\bullet+}$, and **1a**$^{\bullet-}$ on mesolysis generates $R_3Si^{\bullet}$ and $PhSe^-$ species. This efficient dissociation pattern of **1a**$^{\bullet-}$ led us to envisage the utilization of −Si−Se− bonds in general as silyl radical equivalents, and hence, we decided to explore the synthetic potentials of such fragmentations for BMGT[35] radical reactions, as PhSeSePh, a good radical trapping agent,[46] is produced in the process. Most of the existing methodologies for radical reactions are based on tin hydride,[47,48] despite its inherent limitations such as toxicity and difficulty in removing tin byproducts. The serious disadvantage of the tin hydride system lies in the loss of functionality due to the termination of radical sequence by hydrogen abstraction and reduction of the starting radical under normal experimental conditions. Although some partial solutions to these problems have been addressed by introducing rather expensive reagents,[49−51] atom transfer approach,[52] or utilizing modified tin-based reagents,[53,54] a practical solution to this problem has remained elusive.

(44) Murov, S. L. *Hand Book of Photochemistry*; Marcel Dekker: New York, 1973; p 124.

(45) The corresponding quantum yield value for the disappearance of **1a** with DMN is observed to be less when compared with DMA. This difference could be possibly due to the competitive ground-state light absorption of **1a** at 310 nm.

(46) (a) Newcomb, M.; Marquardt, D. J.; Kumar, M. U. *Tetrahedron* **1990**, *46*, 2345. (b) Byers, J. H.; Gleason, T. G.; Knight, K. S. *J. Chem. Soc., Chem. Commun.* **1991**, 354.

(47) (a) Giese, B. *Radicals in Organic Synthesis: Formation of Carbon−Carbon Bonds*; Pergamon Press: Oxford, 1986. (b) Beckwith, A. L. J.; Westwood, S. W. *Tetrahedron* **1989**, *45*, 5269. (c) Ramaiah, M. *Tetrahedron* **1987**, *43*, 3541. (d) Pereyer, M.; Quintard, J.-P.; Rahm, A. *Tin in Organic Synthesis*; Butterworths: London, 1987; Part 2.

(48) (a) Curran, D. P.; Fevig, T. L.; Jasperse, C. P. *Chem. Rev.* **1991**, *91*, 1237. (b) Curran, D. P. *Synthesis* **1988**, 417, 489.

(49) Clark, K. B.; Griller, D. *Organometallics* **1991**, *10*, 746 and references therein.

(50) Giese, B. *Angew. Chem., Int. Ed. Engl.* **1985**, *24*, 553 and references therein.

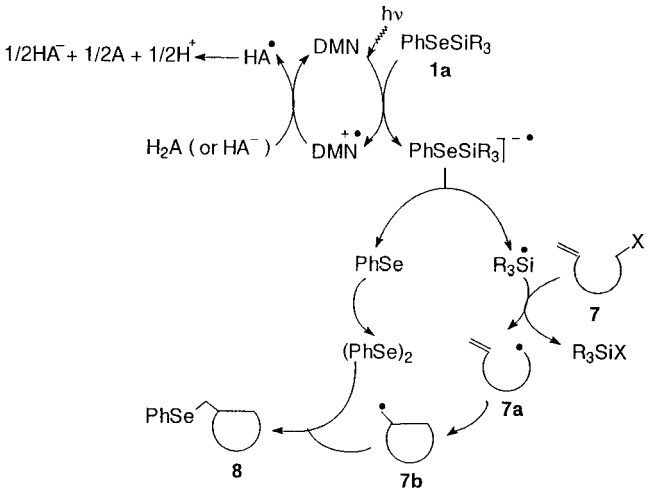

Figure 10. Complete photocycle for PET-initiated BMGT radical reactions.

Scheme 11

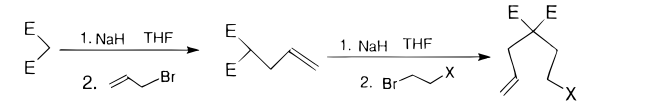

E = $COOC_2H_5$

9. X = Br (yield = 79%)
11. X = Cl (yield = 90%)

Since our study, as described above (Scheme 9), has suggested the easy generation of silyl radicals and PhSeSePh−, a good radical terminating agent, (formed by the oxidative dimerization[55] of $PhSe^-$) in one pot by the PET reductive activation of **1a**, it was envisaged that this chemistry could be utilized for the group-transfer radical reactions as depicted in Figure 10.

Initially, substrate **9** was chosen to evaluate the applicability of **1a** as a reagent for BMGT radical reactions. **9** was prepared in 79% yield by the sequential alkylation of in situ generated diethyl malonate anion, with allyl bromide (21 mmol) and 1,2-dibromoethane (15 mmol), respectively (Scheme 11).

PET cyclization of **9** was achieved by irradiating a dilute solution containing a mixture of **9** (1.4 mmol), **1a** (1.4 mmol), DMN (0.55 mmol), and ascorbic acid (1.4 mmol) through Pyrex-filtered light ($\lambda \geq 310$ nm) using a 450 W Honovia medium-pressure mercury vapor lamp at room temperature without removing dissolved oxygen from the solution. The progress of the reaction was monitored by both TLC and HPLC analysis. After 9 h of irradiation, when quantitative consumption of **9** was noticed, irradiation was discontinued. Solvent was removed under vacuum, and the crude photolyzate was purified by silica gel chromatography to give a viscous yellow oily product (**10a**) in 75% yield. Product **10a** was characterized by ^{1}H NMR, ^{13}C NMR, and MS spectral analysis (for details see the Experimental Section). DMN was recovered unchanged in about 98% yield.

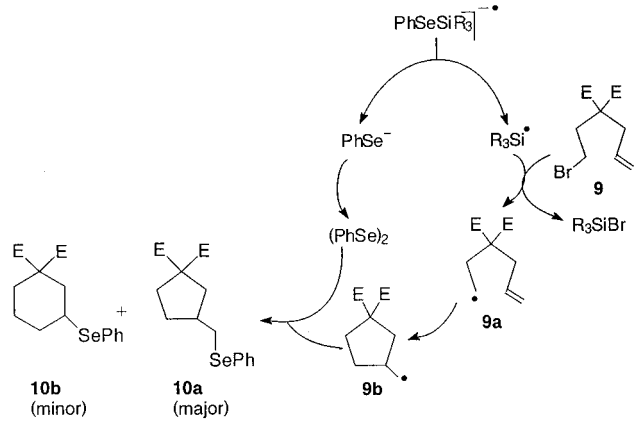

Figure 11. Radical sequences for group-transfer cyclization reactions.

Scheme 12

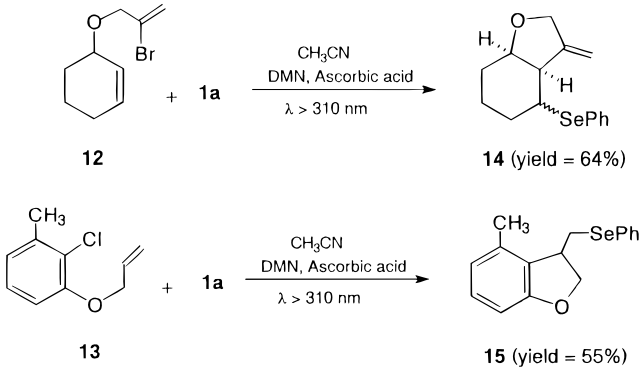

Formation of another minor product (<12% yield, estimated by HPLC analysis) was also observed during the cyclization of **9**; however, this could not be isolated in pure form for complete spectral characterization, but ^{1}H NMR of the crude mixture indicated the possibility of this compound being an *endo-trig* cyclization product (**10b**).

Generally, the carbon-centered radical generation by Bu_3SnH is performed by the reductive cleavage of the −C−Br bond.[47d] The reaction using the −C−Cl bond has been found to be significantly sluggish. Therefore, to compare the −C−Cl bond cleavage efficiency by silyl radical species, compound **11** was also included in our study. Preparative PET reaction of **11**, using an experimental setup identical to that described for **9**, led to the formation of cyclized product **10a** in 63% yield (Figure 11). A comparative rate study for the cyclizations of **9** and **11** suggested both to be comparable. Therefore, it may be suggested that radical chain initiation through this approach could be achieved by employing −C−Cl bonds as well.

To evaluate the effectiveness of PET-generated silyl radical for the generation of vinyl as well as arene radicals, cyclizations of substrates **12** and **13** were also initiated, which furnished **14** and **15** in 63% and 55% yield, respectively (Scheme 12). These products were characterized by ^{1}H NMR, ^{13}C NMR, and MS spectral data.

(51) (a) Chatgilialoglu, C. *Acc. Chem. Res.* **1992**, *25*, 188 and references therein. (b) Chatgilialoglu, C.; Ferreri, C. *Res. Chem. Intermed.* **1993**, *19*, 755. (c) Chatgilialoglu, C.; Ingold, K. U.; Scaiano, J. C. *J. Am. Chem. Soc.* **1982**, *104*, 5123.

(52) (a) Curran, D. P.; Chang, C.-T. *Tetrahedron Lett.* **1987**, *28*, 2477. (b) Curran, D. P.; Chen, M.-H.; Kim, D. *J. Am. Chem. Soc.* **1986**, *108*, 2489.

(53) Zard, S. Z.; Boivin, J.; Camara, J. *J. Am Chem. Soc.* **1992**, *114*, 7909.

(54) (a) Keck, G. E.; Yates, J. B. *J. Am. Chem. Soc.* **1982**, *104*, 5821. (b) Keck, G. E.; Enholm, E. J.; Yates, J. B.; Wiley, M. R. *Tetrahedron* **1985**, *41*, 4079.

(55) Foster, D. G. *Organic Synthesis*; Wiley: New York, 1955; Collect. Vol. 3, p 771.

Table 1. Bimolecular Group Transfer Radical Reactions[a]

Entry	Substrate[i]	Product[ii]	*cis / trans* or *E/Z*[iii,iv]	Yield[v] (%)
1.	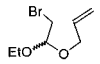 **16**	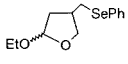 **23**	16 / 84	81
2.		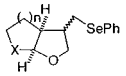		84
	17. n = 2 ; X = O	**24**	82 / 18	87
	18. n = 1 ; X = CH_2	**25**	70 / 30	82
	19. n = 2 ; X = CH_2	**26**	75 / 25	77
3.	 **20**	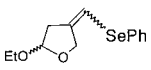 **27**	32 / 68	75
4.		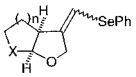		
	21. n = 2 ; X = O	**28**	88 / 12	72
	22. n = 1 ; X = CH_2	**29**	66 / 34	70

[a] Key: (i) see the Supporting Information for the preparation and characterization of **16**−**22**; (ii) characterized by ^{1}H NMR, ^{13}C NMR, and mass spectral analyses; (iii) cis/trans and *E*/*Z* ratios are confirmed by using HPLC; isomers were not separable by column chromatography; (iv) in the case of **24** and **28** only the major isomer was isolated; the minor isomer was not obtained in enough quantity for spectral characterization; (v) isolated yields, but not optimized.

Generality of BMGT Reactions. To test the generality and applicability of **1a** as a bimolecular group transfer reagent, preparative cyclizations of a series of bromoallyl ethers **16**−**19** and bromopropargyl ethers **20**−**22** were undertaken, and the results are presented in Table 1. Spectral details of the cyclic products **23**−**29** are presented in the Experimental Section.

Intermolecular Radical Addition Reactions. Encouraged by the success in conducting BMGT radical cyclization reactions using **1a** as reagent, we diverted our attention using this protocol toward intermolecular group transfer radical chain addition reactions. Although much attention have been focused on radical cyclization reactions, intermolecular radical chain addition reactions have remained unexplored due to the possible competing hydrostannation reaction of electron-deficient alkenes using conventional trialkyltin reagent as initiator.[48b] Furthermore, the primary alkyl radical formed by the cleavage of the −C−X (X = halogen) bond has two possible options for termination with similar rate constants either by hydrogen atom abstraction from tin hydride or by addition to an electron-deficient alkene. Although the addition of alkyl radicals to an alkene can be directed to some extent by using excess of olefin, the coupling of adduct radicals with another molecule of alkene leads to the formation of telomers and polymers.[48b] Despite these limitations, the unique features of radical additions make them useful, and some intermolecular radical additions are precedented in the literature.[56−58]

In this context, we evaluated the expansion of the scope of our methodology (Figure 10) for intermolecular radical-chain addition reactions. It was envisioned that the polymerization problem, normally observed during intermolecular radical additions using tributyltin hydride reagent, could be avoided as the termination step in this case (Figure 12) involves fast phenylselenyl group transfer rather than H atom transfer. Toward this endeavor, we desired to study the addition of $^{\bullet}CH_2CO_2C_2H_5$ [from the precursor bromoethylacetate (**30**)] across the C=C bond of **31**. Substrate **31** was prepared by following the simple steps as shown in Scheme 13.

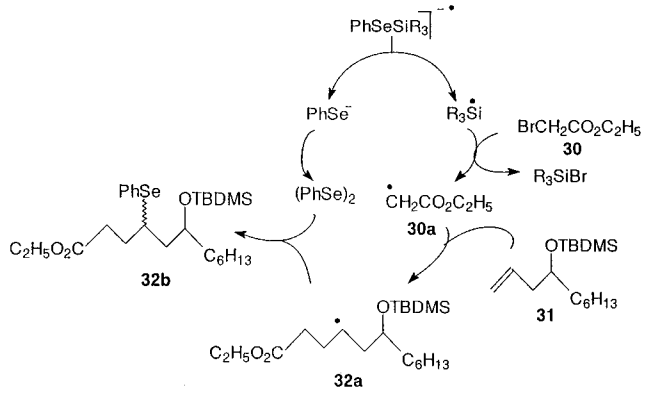

Figure 12. Radical chain sequences for intermolecular-chain addition reactions.

Scheme 13

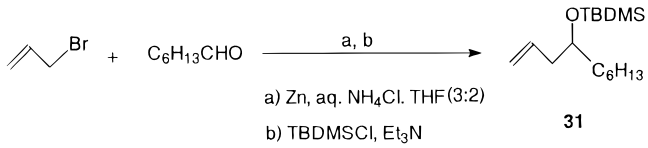

Usual PET reaction of a dilute solution of acetonitrile containing a mixture of **1a** (1.6 mmol), DMN (0.5 mmol), ascorbic acid (1 mmol), **31** (1.8 mmol), and **30** (2.3 mmol) furnished a yellow oily product in 55% yield. The product was characterized as **32b** by ^{1}H NMR, ^{13}C NMR, and mass spectral analysis (for details see the Experimental Section).

Conclusion

In conclusion, we have developed a conceptually new photosystem to drive PET reductive activation of −Si−Se− bonds. Although preliminary studies such as steady-state photolysis experiments indicated the ET processes from DMN or DMA to −Si−Se− bonds, a keen insight on the mechanistic understanding is obtained from picosecond and nanosecond laser flash photolysis studies. The synthetic potential of $\mathbf{1a}^{\bullet-}$ mesolysis is explored in BMGT radical reactions and intermolecular group transfer chain addition reactions. This study adds a new dimension in the radical chemistry from a conceptual and ecological viewpoint.

Experimental Section

General Methods. DMN,[37] DMA,[39] and PhSeSePh[59] were synthesized and purified following the literature procedures. Cyclohexane and acetonitrile that are used in fluorescence

(56) (a) Giese, B.; Gonzalez-Gomez, J. A.; Witzel, T. *Angew. Chem., Int. Ed. Engl.* **1984**, *23*, 69. (b) Giese, B. *Ibid.* **1983**, *22*, 753.

(57) (a) Curran, D. P.; Eichenberger, E.; Collis, M.; Roepel, M. G.; Thoma, G. *J. Am. Chem. Soc.* **1994**, *116*, 4279. (b) Curran, D. P.; Thoma, G. *Ibid.* **1992**, *114*, 4436.

(58) (a) Byer, J. H.; Lane, G. C. *J. Org. Chem.* **1993**, *58*, 3355. (b) Byer, J. H.; Harper, B. C. *Tetrahedron Lett.* **1992**, *33*, 6953.

studies and HPLC analysis, respectively, were of spectroquality (E. Merck, India) grade. Silica gel for column chromatography (finer than 200 mesh) was obtained from Acme, India.

All nuclear magnetic resonance spectra were recorded on either Bruker AC 200 FT NMR or Brucker MSL 300 NMR spectrometers using $CDCl_3$ as solvent. All chemical shifts are reported in parts per million downfield from TMS; coupling constants are given in hertz. IR spectra were taken on a Perkin-Elmer model 2830 spectrometer. Mass spectra were obtained at a voltage of 70 eV on a Finnigan MAT-1020B instrument.

Fluorescence lifetimes were measured using the time-resolved fluorescence spectrometer (model 199 from Edingburgh Instruments, U.K.), which uses a hydrogen-discharge flash lamp providing pulses of 1 ns duration for excitation and single-photon-counting techinque for detection.

Fluorescence spectra were recorded on a Spex-Fluorolog 212 spectrofluorimeter. The excitation and emission slit widths were maintained at 0.5 mm. The steady-state emission spectral measurements were carried out using a 1 cm × 1 cm quartz cell. A right angle configuration for the cell holder was utilized during the measurement of excitation and emission spectra.

The linear accelarator used in pulse radiolysis experiments was obtained from M/S Viritech Ltd., U.K.

A mode-locked Nd:YAG laser was used for excitation purporses in picosecond and nanosecond laser flash photolysis experiments.

HPLC analysis was performed on a Perkin-Elmer (model 250 binary LC pump along with LC 135C diode array detector) liquid chromotograph using reversed-phase C_{18} (bondapack 0.5 μm) column, eluting with CH_3CN/H_2O (75:25) solvent mixture degassed by a freeze−thaw cycle procedure.

Cyclic Voltammetry. The cyclic voltammetry experiments were carried out with a three-electrode assembly on a PAR 175 universal programmer and PAR RE0074 XY recorder. The cell consisted of a Metro E410 hanging mercury drop electrode (HMDE) and Pt wire (auxiliary electrode). The supporting electrolyte was tetraethylammonium perchlorate, and potentials are referred to SCE and are uncorrected for liquid junction potentials.

Steady-State Fluorescence Quenching. Quenching of DMN or DMA fluorescence was carried out by using **1a** as quencher. For the determination of Stern−Volmer constants (K_{qf}SS), the intensity (I_0) of steady-state fluoresence at the maximum emission (λ_{emi}(DMN) = 344 nm; λ_{emi}(DMA) = 440 nm) was measured from DMN/DMA solution (3×10^{-4} M) in CH_3CN at 25 °C, keeping the excitation wavelength (λ_{exi}) at 310 nm for DMN and 410 nm for DMA. Subsequently, the fluoresence-quenching intensity (I) was measured as a function of concentration [Q] of **1a**. Linear plots were obtained on the basis of the equation $I_0/I = 1 + K_{qf}\tau$[Q], where I_0 denotes the fluoresence intensity in the absence of quencher. No curvature was noticed in any system, and intercepts were 1.05 ± 0.007 in all cases. Slopes were determined by least-squares fit, and coefficients were always >0.99.

Pulse Radiolysis. High-energy (7 meV) electron pulses of 50 ns duration generated from a linear electron accelerator (LINAC) were used for pulse radiolysis experiments. The details of the pulse radiolysis setup have been described elsewhere.[60] The transient species produced were detected by monitoring the optical absorption. The absorbed dose was determined by using the aerated KSCN solution $G\epsilon = 21\,520$ $dm^3\ mol^{-1}\ cm^{-1}$ for 100 eV of absorbed dose (the G value is the number of radicals or molecules produced per 100 eV of absorbed energy and ϵ is the molar absorptivity at 500 nm for the transient $(SCN)_2^{\bullet -}$.

Laser Flash Photolysis. The laser flash photolysis experimental setup has been described elsewhere.[61] In brief, the third (355 nm, 5 mJ) harmonic output pulses of 35 ps duration from an active passive mode-locked Nd:YAG laser (Continuum, Model 501-C-10) used for excitation and continuum probe pulses in the 400−920 nm region were generated by focusing the residual fundemental in the H_2O/D_2O mixture (50:50). The probe was delayed with respect to the pump pulse using a 1 m long linear motion translation stage, and the transient absorption spectra at different delay times (up to 6 ns) were recorded by an optical multichannel analyzer (Spectroscopic Instruments, Germany) interfaced to an IBM-PC. At the zero delay position, the probe light reaches the sample just after the end of the pump pulse. Transients surviving beyond 50 ns were studied by monitoring their absorption using a tungsten filment lamp in combination with a Bausch and Lomb monochromator (f/10, 350−800 nm), Hamamatsu R 928 PMT, and a 500 MHz digital oscilloscope (Tektronix, TDS-540A) connected to a PC.

Quantum Yield Measurements. Samples for the quantum yield determinations were prepared by pipetting out a noted volume from the stock solution of **1a** into Pyrex tubes and irradiated in a Quantum yield reactor (Model QYR-20) using a 200 W mercury lamp. Irradiations were carried out for a short interval of time to bring about only 8−10% of the conversion. A uranyl oxalate actinometer was used to monitor the intensity of light. The quantitative loss of **1a** was estimated by HPLC [column: C_{18} , eluent: CH_3CN/H_2O (3:1)]. The limiting quantum yield (ϕ_{lim}) for **1a** was obtained from the inverse plot of the variable **1a** concentrations vs quantum yields i.e., $[\mathbf{1a}]^{-1}$ vs ϕ_{dis}^{-1}, by keeping the DMN/DMA concentration fixed.

Preparation of *tert*-Butyldiphenyl(phenylseleno)-silane (1a).[36] A solution of diphenyl diselenide (15.6 g, 0.05 mol) in 100 mL of dry THF was added to freshly prepared sodium sand (3 g, 0.14 mol), and the resulting mixture was refluxed for 5 h. *tert*-Butyldiphenylsilyl chloride (27.5 g, 0.1 mol) was added to the stirring solution, and the resulting mixture was allowed to reflux for 21 h. The reaction mixture was cooled to 0 °C, and 5 mL of methanol was added to kill the excess of sodium. The reaction mixture was extracted with 100 mL of ether, washed with several portions of cold water, dried over sodium sulfate, and concentrated under reduced pressure. Distillation of the crude reaction mixture gave 30 g (79%) of **1a** as thick pale yellow liquid, which on long standing (24 h) solidified: mp = 57 °C (lit.[36] mp 56−58 °C); IR (KBr) 3038, 2910, 2840, 1563, 805, 720, 660 cm^{-1}; ^1H NMR (200 MHz) δ 7.64 (m, 4H), 7.29 (m, 6H), 6.98 (m, 5H), 1.14 (s, 9H); MS 396 (M^+).

PET Activation of 1a Using DMN as Sensitizer. A dilute solution of acetonitrile (300 mL) containing a mixture of **1a** (0.120 g, 0.3 mmol), DMN (0.070 g, 0.1 mmol), and ascorbic acid (0.05 g, 0.3 mmol) was irradiated through Pyrex-filtered light ($\lambda \geq 310$ nm) using a 450 W Hanovia medium-pressure lamp at room temperature. The progress of the reaction was monitored by HPLC (C_{18} reversed-phase column: CH_3CN/H_2O = 70:30) analysis. After 5 h of irradiation, when considerable consumption of **1a** was noticed, irradiation was discontinued, and solvent was removed under vacuum. The crude reaction mixture was purified by column chromatography to give **5** and **6**. The products (**5** and **6**) were characterized by comparing their spectral data with the reported values. DMN was recovered unchanged after the reaction in about 98% yield.

Visible-Light PET Activation of 1a Using DMA as Sensitizer. PET activation of **1a** by visible light (410 nm) using DMA as the electron donor also led to the formation of **5** and **6** in more or less the same proportions. This reaction was performed in a specially designed double-walled photoreactor. The photoreactor consisted of three chambers. The first and outermost chamber contained irradiation solution, while the second one was charged with a $CuSO_4 \cdot 5H_2O/NH_3$ filter solution. This filter solution allowed only the 410 nm wavelength light to pass through.[31] A 450 W Hanovia medium-pressure mercury lamp was used as the light source and was housed into a water-circulated double-jacketed chamber im-

(59) Hori, T.; Sharpless, K. B. *J. Org. Chem.* **1978**, *43*, 1689.
(60) Guha, S. N.; Moorthy, P. N.; Kishore, K.; Naik, D. B.; Rao, K. N. *Proc. Indian. Acad. Sci. (Chem. Sci.)* **1989**, *99*, 261.
(61) Ghosh, H. N.; Sapre, A. V.; Palit, D. K.; Mittal, J. P. *J. Phys. Chem. B* **1997**, *101*, 2315.

mersed in the second chamber, maintaining 1 cm path length of the filter solution. The whole photoreactor was made of Pyrex glass.

General Irradiation Procedure for the PET-Promoted Radical Chain Group Transfer Reactions. Method A. Using DMN as Sensitizer. This is illustrated by taking **9** as an example.

A dilute solution containing a mixture of **9** (0.43 g, 1.4 mmol), **1a** (0.55 g, 1.4 mmol), DMN (0.13 g, 0.55 mmol), and ascorbic acid (0.25 g, 1.4 mmol) was irradiated through Pyrex-filtered light ($\lambda \geq 310$ nm) using a 450 W Honovia medium-pressure mercury vapor lamp at room temperature without removing dissolved oxygen from the solution. The progress of the reaction was monitored both by TLC and HPLC analysis. After 9 h of irradiation, when quantitative consumption of **9** was noticed, irradiation was discontinued. Solvent was removed under vacuum, and the crude photolyzate was purified by silicagel chromatography to give 0.39 g of a viscous yellow oily product (**10a**) in 75% yield. The product **10a** was characterized by ^{1}H NMR, ^{13}C NMR, and mass spectral analysis, and the data are as follows: IR (neat) 3070, 2860, 1710 cm^{-1}; ^{1}H NMR (200 MHz) δ 1.25 (t, 6H, J = 9.75 Hz), 1.45 (m, 1H), 1.90 (m, 2H), 2.25 (m, 3H), 2.55 (m, 1H), 2.95 (d, 2H, J = 4.75 Hz), 4.20 (q, 4H, J = 9.75 Hz), 7.25 (m, 3H), 7.55 (m, 2H); ^{13}C NMR (75.47 MHz): δ 172.57, 132.96, 129.27, 127.06, 61.61, 60.41, 40.94, 40.24, 34.06, 33.48, 32.64, 14.27; MS *m/e* (rel intensity) 384 (M$^+$, 18), 339 (7), 227 (52), 119 (27), 153 (100), 79 (28). Anal. Calcd for $C_{18}H_{24}O_4Se$: C, 56.39; H, 6.31. Found: C, 56.34; H, 6.29.

Identical irradiation of substrates **11**−**13** and **16**−**22** gave **10a**, **14**, **15**, and **23**−**29**, respectively. The spectral details of **14**, **15**, and **23**−**29** are as follows.

Compound 14: IR (neat) 3050, 1620, 1550, 1460, 1210 cm^{-1}; ^{1}H NMR (200 MHz) δ 1.80−1.60 (m, 4H), 2.25−2.35 (m, 2H), 2.55−2.60 (m, 1H), 3.00 (m, 1H), 3.55 (m, 2H), 4.30−4.15 (m, 1H), 5.80 (d, 2H, J = 4.5 Hz), 7.25 (m, 3H), 7.55 (m, 2H); ^{13}C NMR (75.47 MHz) δ 147.21, 136.81, 135.40, 130.29, 128.93, 109.26, 79.62, 71.97, 50.21, 43.83, 33.15, 30.97, 26.35; MS *m/e* (rel intensity) 294 (M$^+$, 10), 238 (5), 157 (8), 125 (75), 107 (60), 81 (100).

Compound 15: IR (neat) 1590, 1470, 1230 cm^{-1}; ^{1}H NMR (200 MHz) δ 2.15 (s, 3H), 3.10 (m, 2H), 3.30 (m, 1H), 4.80 (d, 2H, J = 7.5 Hz), 6.75 (t, 1H, J = 7.5 Hz), 6.95 (dd, 2H, J = 7.5, 16.5 Hz), 7.25 (m, 3H), 7.55 (m, 2H); ^{13}C NMR (50.32 MHz) δ 157.77, 133.00, 129.65, 129.30, 129.10, 127.24, 125.42, 122.34, 120.48, 119.59, 81.53, 37.70, 32.70, 15.11; MS *m/e* (rel intensity) 304 (M$^+$, 25), 172 (10), 157 (10), 147 (100).

Compound 23: IR (neat) 3070, 1200, 1125 cm^{-1}; ^{1}H NMR (200 MHz, $CDCl_3$) δ 1.20 (t, 3H J = 9.7 Hz), 1.75 (m, 1H), 2.20−2.50 (m, 2H), 3.00 (m, 2H), 3.45 (m, 1H), 3.75 (m, 2H), 4.05 (t, 1H, J = 9.7 Hz), 5.15 (m, 1H), 7.25 (m, 3H), 7.55 (m, 2H); ^{13}C NMR (50.32 MHz, $CDCl_3$) δ 132.97, 131.60, 130.00, 129.26, 129.18, 127.79, 127.09, 104.20, 104.01, 72.04, 62.99, 62.78, 39.86, 39.64, 38.67, 37.91, 32.33, 31.54, 15.42, 15.33; MS *m/e* (rel intensity) 286 (M$^+$, 286), 240 (15), 157 (23), 91 (42), 83 (100). Anal. Calcd for $C_{13}H_{18}O_2Se$: C, 54.74; H, 6.36. Found: C, 54.53; H, 6.38.

Compound 24: IR (neat) 3085, 1210, 1122 cm^{-1}; ^{1}H NMR (200 MHz, $CDCl_3$) δ 1.60 (m, 4H), 2.15 (m, 1H), 2.65 (m, 1H), 2.95 (m, 2H), 3.70 (m,3H), 4.05 (t, 1H, J = 7.15 Hz), 5.25 (d, 1H, J = 4.3 Hz), 7.30 (m, 3H), 7.55 (m, 2H); ^{13}C NMR (75.47 MHz, $CDCl_3$) δ 132.90, 129.33, 128.95, 127.04, 101.62, 69.92, 60.90, 40.93, 37.21, 25.60, 22.80, 19.05; MS *m/e* (rel intensity) 298 (M$^+$, 6), 197 (20), 157 (12), 141 (51), 116 (42), 95 (33), 77 (55), 69 (88), 55 (100). Anal. Calcd for $C_{14}H_{18}O_2Se$: C, 56.57; H, 6.10. Found: C, 56.45; H, 6.11.

Compound 25 : IR (neat) 3080, 1615, 1125 cm^{-1}; ^{1}H NMR (200 MHz, $CDCl_3$) δ 1.65−1.85 (m, 4H), 2.10−2.25 (m, 3H), 2.60 (m, 1H), 3.00 (m, 2H), 3.45 (m, 1H), 3.95 (m, 1H), 4.55 (m, 1H), 7.30 (m, 3H), 7.55 (m, 2H); ^{13}C NMR (75.47 MHz, $CDCl_3$) δ 132.88, 132.54, 130.25, 130.03, 129.02, 126.98, 126.84, 86.18, 85.15, 73.31, 72.17, 50.07, 47.97, 47.04, 43.37, 34.46, 34.01, 32.32, 30.73, 26.34, 25.93, 25.21, 24.05; MS *m/e* (rel intensity) 282 (M$^+$, 10), 157 (15), 124 (17), 107 (20), 95 (75), 67 (100). Anal. Calcd for $C_{14}H_{18}OSe$: C, 59.79; H, 6.45. Found: C, 59.55; H, 6.43.

Compound 26: IR (neat): 3080, 1615, 1125 cm^{-1}. ^{1}H NMR (200 MHz): δ 1.65−1.85 (m, 9H), 2.60 (m, 1H), 3.00 (m, 2H), 3.45 (m, 1H), 3.95 (m, 1H), 4.55 (m, 1H), 7.30 (m, 3H), 7.55 (m, 2H). ^{13}C NMR (75.47 MHz): δ 133.18, 132.77, 130.55, 130.13, 128.88, 127.05, 126.77, 86.45, 85.78, 73.53, 72.34, 50.16, 48.15, 47.25, 43.58, 34.64, 34.18, 32.52, 30.81, 26.54, 26.14, 25.32, 24.25. MS *m/e* (relative intencity): 296 (M$^+$, 10), 157 (15), 139 (29), 77 (52).

Compound 27: IR (neat) 3085, 1620, 1200, 1129 cm^{-1}; ^{1}H NMR (200 MHz, $CDCl_3$) δ 1.25 (t, 3H, J = 8.1 Hz), 2.75 (m, 2H), 3.50 (m, 1H), 3.80 (m, 1H), 4.50 (m, 2H), 5.35 (m, 1H), 6.40 (m,1H), 7.25 (m, 3H), 7.55 (m, 2H); ^{13}C NMR (50.32 MHz, $CDCl_3$) δ 145.24, 143.83, 131.55, 131.29, 131.16, 129.24, 127.73, 126.89, 126.80, 108.44, 107.59, 103.51, 69.66, 69.44, 62.79, 62.65, 40.73, 39.60, 15.26; MS *m/e* (rel intensity) 284 (M$^+$, 1), 157 (15), 129 (100), 115 (23), 91 (16). Anal. Calcd for $C_{13}H_{16}O_2Se$: C, 55.13; H, 5.69. Found: C, 54.89; H, 5.71.

Compound 28: IR (neat) 3085, 1625, 1200, 1129 cm^{-1}; ^{1}H NMR (300 MHz, $CDCl_3$) δ 1.65 (m, 3H), 2.30−2.55 (m, 2H), 3.50 (m, 1H), 3.80 (m, 1H), 4.50 (m, 2H), 5.35 (m, 1H), 6.40 (s, 1H), 7.25 (m, 3H), 7.55 (m, 2H); ^{13}C NMR (50.32 MHz, $CDCl_3$) δ 144.97, 132.85, 129.03, 128.99, 127.33, 101.55, 69.95, 61.05, 41.21, 25.06, 23.12; MS *m/e* (rel intensity) 296 (M$^+$, 7), 157 (18), 139 (100), 125 (22), 91 (28). Anal. Calcd for $C_{14}H_{16}O_2Se$: C, 56.96; H, 5.46. Found: C, 56.79; H, 5.44.

Compound 29: IR (neat) 3085, 1645, 1210 cm^{-1}; ^{1}H NMR (200 MHz, $CDCl_3$) δ 1.60−1.75 (m, 6H), 2.75 (m, 1H), 3.60 (m, 2H), 4.05 (t, 1H, J = 4.3 Hz), 6.65 (m, 1H), 7.30 (m, 3H), 7.55 (m, 2H); ^{13}C NMR (75.47 MHz, $CDCl_3$) δ 145.75, 146.01, 133.12, 133.99, 129.75, 129.30, 129.04, 117.75, 117.23, 83.02, 82.95, 74.45, 73.82, 46.15, 45.99, 37.91, 37.72, 33.35, 32.47, 26.75, 25.21; MS *m/e* (rel intensity) 280 (M$^+$, 3), 157 (16), 123 (100), 109 (20), 91 (15). Anal. Calcd for $C_{14}H_{16}OSe$: C, 60.22; H, 5.78. Found: C, 59.99; H, 5.76.

Method B. Using DMA as Sensitizer. Identical irradiations (for the substrates **9**, **11**−**13**, and **16**−**22**) as described in method A were carried out using DMA as sensitizer at 410 nm wavelength light, in a specially designed photoreactor (see Visible Light PET Activation of **1a**). Similar products (**10a**, **14**−**15**, and **23**−**29**) were obtained in more or less the same proporations.

Intermolecular Radical Chain Addition Reaction. Identical PET reaction of a dilute solution of acetonitrile containing a mixture of **1a** (0.55 g, 1.4 mmol), DMN (0.1 g, 0.5 mmol), ascorbic acid (0.18 g, 1 mmol), **30** (0.38 g, 2.3 mmol), and **31** (0.49 g, 1.8 mmol) furnished a yellow oily product in 55% yield (0.32 g). The product **32b** was characterized by ^{1}H NMR, ^{13}C NMR, and mass spectral analysis, and the data are as follows.

Compound 32b: IR (neat) 1710, 1580, 1420 cm^{-1}; ^{1}H NMR (200 MHz) δ 0.10 (s, 9H), 0.95 (t, 3H, J = 7.5 Hz), 1.45 (m, 3H), 1.25 (m, 10H), 1.95 (dd, 2H, J = 4.5, 8.5 Hz), 2.55 (1H), 3.15 (m, 1H), 4.10 (2H, J = 7.5 Hz), 7.25 (m, 3H), 7.55 (m, 2H); ^{13}C NMR (75.47 MHz) δ 173.05, 135.64−127.25, 70.5, 70.4, 60.16, 43.5, 42.32, 41.99, 37.75−29.33, 25.84, 25,78, 24.68, 24.62, 22.42, 17.93, 14.1, −4.1, −4.4; MS *m/e* (rel intensity) 514 (M$^+$, 4), 244 (100), 457 (18), 171 (30), 157 (20).

Acknowledgment. This work was partly supported by BRNS, Bombay, India. One of us (K.S.S.P.R.) thanks BARC, Bombay, India, for the award of the Dr. K. S. Krishnan fellowship.

Supporting Information Available: Experimental procedures and spectral characterization of **9**, **11**−**13**, **16**−**22**, and **31** (5 pages). This material is contained in libraries on microfiche, immediately follows this article in the microfilm version of the journal, and can be ordered from the ACS; see any current masthead page for ordering information.

JO972345E